Journal of Hydrology 495 (2013) 238–251

Contents lists available at SciVerse ScienceDirect

Journal of Hydrology

journal homepage: www.elsevier.com/locate/jhydrol

Integrated flow and temperature modeling at the catchment scale

Maria C. Loinaz [a,*], Hasse Kampp Davidsen [a], Michael Butts [b], Peter Bauer-Gottwein [a]

[a] Technical University of Denmark, Department of Environmental Engineering, 2800 Kgs. Lyngby, Denmark
[b] DHI, Agern Alle 5, DK-2970 Hørsholm, Denmark

ARTICLE INFO

Article history:
Received 29 March 2012
Received in revised form 18 April 2013
Accepted 22 April 2013
Available online 6 May 2013
This manuscript was handled by Peter K. Kitanidis, Editor-in-Chief, with the assistance of Hongbin Zhan, Associate Editor

Keywords:
Stream temperature
Integrated surface water–groundwater modeling
Idaho
Silver Creek

SUMMARY

Changes in natural stream temperature levels can be detrimental to the health of aquatic ecosystems. Water use and land management directly affect the distribution of diffuse heat sources and thermal loads to streams, while riparian vegetation and geomorphology play a critical role in how thermal loads are buffered. In many areas, groundwater flow is a significant contribution to river flow, particularly during low flows and therefore has a strong influence on stream temperature levels and dynamics. However, previous stream temperature models do not properly simulate how surface water–groundwater dynamics affect stream temperature. A coupled surface water–groundwater and temperature model has therefore been developed to quantify the impacts of land management and water use on stream flow and temperatures. The model is applied to the simulation of stream temperature levels in a spring-fed stream, the Silver Creek Basin in Idaho, where stream temperature affects the populations of fish and other aquatic organisms. The model calibration highlights the importance of spatially distributed flow dynamics in the catchment to accurately predict stream temperatures. The results also show the value of including temperature data in an integrated flow model calibration because temperature data provide additional constraints on the flow sources and volumes. Simulations show that a reduction of 10% in the groundwater flow to the Silver Creek Basin can cause average and maximum temperature increases in Silver Creek over 0.3 °C and 1.5 °C, respectively. In spring-fed systems like Silver Creek, it is clearly not feasible to separate river habitat restoration from upstream catchment and groundwater management.

1. Introduction

Watershed management to optimize the health of the freshwater biotic community is becoming increasingly recognized as a necessary concept for achieving sustainability (Haper et al., 2008). Ecohydrology is a relatively new discipline within water management, which studies the functional interrelations between hydrology and biota at the catchment scale (Zalewski, 2000). Thus, the development of integrated ecohydrologic tools that can effectively relate the physical environment to measures of ecological status, and be applied at the catchment scale, is one of the most important challenges for the water resources community.

Temperature is a critical factor in defining the distribution of stream ecosystems and in determining the metabolic rates of organisms and their ability to interact with other species (Allan and Castillo, 2007). High stream temperatures can cause impaired growth and increased predation rates in certain aquatic species (Roth et al., 2010). Moreover, water temperature is the most important factor in fish reproduction (Fujimoto et al., 2008). Temperature serves as an indicator of water quality and ecosystem status, particularly fish habitat suitability. Therefore, the accurate simulation of stream water temperature in a catchment is an important goal in the context of ecohydrology.

Previous modeling work on heat loads in rivers was motivated by the impact of thermal loads from power plants (Butz et al., 1974; Jackman and Yotsukura, 1977; Kinzelbach, 1981; Poulin and Hubert, 1982). However, in many catchments heat loads to streams are dominated by diffuse sources rather than point sources. Thermal loads from diffuse sources may come from urban or agriculture runoff, and can be influenced by changes in natural drainage patterns and geomorphology, as well as changes in water use, land use, and vegetation. This study is focused on the impact of diffuse heat loads rather than heat point sources.

Stream temperature variations can be influenced by watershed management, such as surface and groundwater use, land use and vegetation management; often these catchment parameters are interrelated (Boyd and Kasper, 2003). Solar radiation is the most important source of heat to rivers during most of the year (Beschta, 1997; Boyd and Kasper, 2003). Removal of vegetation can significantly increase stream temperatures by increasing incoming radiation (Roth et al., 2010) as well as accelerate bank erosion, which can widen the stream channel. Increasing surface area and decreasing channel depth due to sediment accumulation, change river morphology, an important factor that affects stream temperatures (Klein et al., 2007). Water depth and flow volume influence the

* Corresponding author. Tel.: +1 727 592 8062.
E-mail address: mcloinaz@gmail.com (M.C. Loinaz).

0022-1694/$ - see front matter © 2013 Elsevier B.V. All rights reserved.
http://dx.doi.org/10.1016/j.jhydrol.2013.04.039

thermal inertia of the water body, which affects the amplitude of diurnal variations and the time lag to reach equilibrium temperature (Gu et al., 1998; Webb et al., 2003). The surface area of the stream affects the amount of heat exchange with the atmosphere and the time it takes to change the temperature of the water, given a certain heat flux (Larson and Larson, 1996). In addition, the surface area or the width of the channel affects the fraction of shade from stream bank vegetation or topography that covers a stream segment (Chen et al., 1998).

The flow regime in a channel has a direct impact on the thermal response of the stream. Several studies have quantified the relationship between flow and temperature (Shanley and Peters, 1988; Sinokrot and Gulliver, 2000; Webb et al., 2003). Sinokrot and Gulliver (2000) showed that increases in flow lead to a reduction in the amplitude of the diurnal temperature variation and critically high temperatures are more frequently exceeded under lower flows. Additionally, it is important to evaluate not only the amount of flow, but also the flow source. In rivers where a significant portion of the flow comes from groundwater, decreases in water table can cause temperature changes, especially in low flow periods. Conversely, areas that receive large amounts of runoff from higher temperature sources, such as surface drains, can contribute to high thermal loads downstream.

The spatial distribution of temperature along a river can be an indicator of the spatial variability in stream habitat conditions. River restoration efforts often focus on improving the bank vegetation and the geomorphology of the river, but river habitat conditions are also influenced by the catchment hydrology (Wissmar and Beschta, 1998). For example, changes in land use or water management (such as channelization, artificial ponding, and water diversions) can directly affect the thermal regime of a tributary, which can in turn deliver a high thermal load to the main stream. The simulation of water temperature in an integrated surface–groundwater hydrologic system makes it possible to assess the distribution of thermal loads in a catchment, which is a key step in understanding the impact of land use management on stream ecology.

Numerous types of stream temperature models have been developed over the past few decades; these can be broadly classified as regression, stochastic, and deterministic models (Cassie, 2006). Deterministic models have an advantage in that they can be applied at multiple scales (Cassie, 2006), but most importantly, they can be applied to evaluate management scenarios. For example, a regression model is only valid if the management boundary conditions are unchanged and therefore they cannot be used to simulate the effects of different management strategies.

Several deterministic models that couple stream hydrodynamics to heat transport have been developed in recent decades (Sinokrot and Stephan, 1993; Kim and Chapra, 1997; Younus et al., 2000; Boyd and Kasper, 2003). These models solve the one-dimensional Saint Venant equations for flow and the advection–dispersion equation for heat transport. An important source/sink term in these stream temperature models is the atmospheric heat exchange. Some models also include the sediment heat flux by conduction. However, most of the applications of these models have been limited to the stream scale and include groundwater flow represented as a fixed lateral inflow in one direction. Heat exchange by groundwater advection can be more important than conduction, if groundwater fluxes are large enough (Constantz, 2008). Moreover, Bogan et al. (2003) suggest that groundwater inflows can explain deviations in the relationship between stream temperature and stream equilibrium temperature with the atmosphere. Thus, a potentially important component of the heat balance for some river systems is neglected by such stream temperature models.

In many regions, groundwater flow controls the hydrologic regime of a river and thus, linking the temperature model to integrated surface water–groundwater models becomes important. An integrated model can simulate the dynamic two-way exchange (gains and losses) between surface water and groundwater so that the spatial variability and dynamics of stream hydrology can be better represented. Moreover, an integrated model can quantify the impact of surface and groundwater abstraction in a catchment more explicitly and thus directly and dynamically link the changes in management practices to stream temperature changes. Finally, a valuable aspect of linking a temperature model to an integrated catchment-scale surface water–groundwater model is the strong relationship between the volume and source of flow and temperature. This means that temperature data provide strong constraints on the flow sources and volumes and thus decrease model uncertainty.

In this study, we dynamically couple an integrated surface water–groundwater model to a surface water heat transport model. The flow model simulates 3-dimensional and spatially distributed hydrological processes and it dynamically exchanges flows between surface water and groundwater. The temperature model includes the atmospheric heat balance terms and surface water–groundwater heat exchange flux by both conduction and advection. Although the model has the capability of simulating groundwater temperature we assume a uniform groundwater temperature for the case study presented, primarily due to a lack of sufficient calibration data to parameterize a heat transport model for the groundwater compartment. This modeling approach provides a complete description of the processes that affect stream temperature and can be used to evaluate stream temperature impacts of climate change, land use, and water use changes at the catchment scale.

The capabilities of the modeling approach are illustrated using the Silver Creek case study. The Silver Creek system is a high-profile aquatic ecosystem, located in Idaho, USA. Ecosystem services (e.g., fishing, bird-watching, canoeing, water quality conservation, water supply, wetland buffer areas, etc.) in Silver Creek are highly dependent on surface water–groundwater dynamics. The Silver Creek Preserve managed by The Nature Conservancy hosts over 8000 visitors a year from every US state and 33 countries. Economic studies have shown that the Preserve contributes over 3 million US dollars to the local economy each year. The impact of surface and groundwater use in the catchment can be observed in the Silver Creek flow and temperature, which have affected the populations of fish and other aquatic organisms in this ecosystem. For example, fish kills in 1992 coincided with drought period and high temperatures (Wetzstein et al., 2000). This problem is exacerbated by increased water use. Thus, catchment managers are looking for solutions to achieve ecosystem sustainability.

2. Methodology

In this section, a description of the flow model components followed by the temperature model components is presented. The general modeling chart (Fig. 1) shows the hydrologic processes included in the model. The dashed gray line delineates the compartments that exchange both flow and heat in either one or two directions. The specific model inputs and data used for the case study and model calibration approach are described in Sections 3 and 4.

2.1. Flow modeling

The MIKE SHE code was chosen for this study because it has been widely used for integrated surface water–groundwater

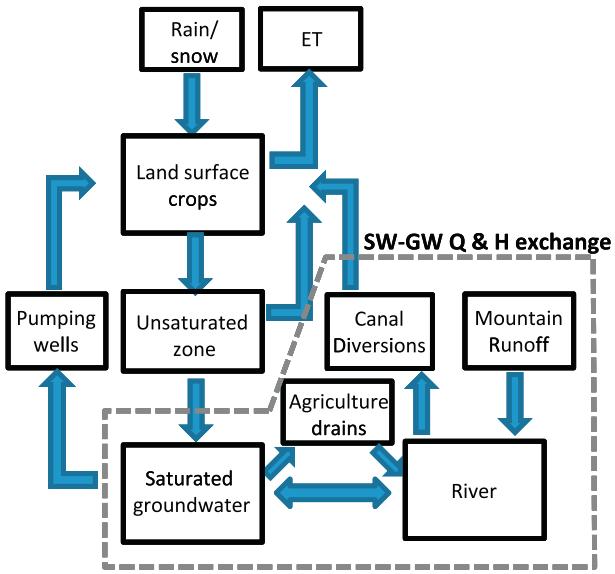

Fig. 1. Model flow chart.

models (Refsgaard et al., 2010; Graham and Butts, 2006) and because it is possible to link the hydrodynamics to water quality processes. MIKE SHE is a physically based and spatially distributed modeling tool for simulating the main processes of the hydrological cycle. Simulated hydrologic processes include snowmelt, interception, overland flow, infiltration into soils, evapotranspiration from vegetation and subsurface flow in the saturated and unsaturated zones (Refsgaard and Storm, 1995). MIKE SHE can be dynamically coupled to MIKE 11, a one-dimensional surface water model that simulates fully dynamic channel flows and control structures (Thompson et al., 2004; Butts et al., 2004).

The main MIKE SHE and MIKE 11 components included in the model are listed below. The equations that describe these processes are found in DHI (2009a) and DHI (2009b).

1. *Precipitation and snow*: the model uses daily input time series data of precipitation and air temperature to calculate rainfall and snowmelt, respectively. Snow dynamics are calculated using a degree-day method (also known as temperature-index method) in which the rate of melting increases as the air temperature increases (Hock, 2003).
2. *Unsaturated zone (UZ) and evapotranspiration (ET)*: the model calculates actual evapotranspiration, infiltration rate, and moisture content of the soils. A relatively simple water balance method (Yan and Smith, 1994) was chosen because it is computationally efficient and more appropriate at the regional scale than the more complex Richards equation approach. The method assumes that all water stored in the root zone is available for transpiration and calculates the average moisture content based on the depth of the water table and the storage capacity of the soil.
3. *The saturated zone (SZ)*: the model uses a finite difference solution to the 3-dimensional Darcy equation for aquifer flow. The SZ module can be spatially discretized vertically and horizontally according to the required complexity. A drainage option is part of the SZ module. Drainage flow occurs when the water table is above a specified elevation. The flow is directly routed to the nearest river or canal in the model at a specified rate.
4. The irrigation module distributes water to crop cells (irrigation command areas) from both the canals and the groundwater according to crop water demand and water availability in the specified sources. The irrigation water is added to the precipitation component, simulating sprinkler irrigation.
5. The MIKE 11 surface water flow model uses a finite difference approach to solve the one-dimensional dynamic wave Saint Venant equations. It calculates water levels and discharges for alternating points along the length of the streams. It also has different types of operating and non-operating control structures (weirs, culverts, gates, and pumps). Exchange flows between the groundwater in MIKE SHE and the MIKE 11 streams occur in the direction of the head gradient and are controlled by specified leakage coefficients for the streambeds.
6. The NAM model in MIKE 11 (Nielsen and Hansen, 1973) is a lumped parameter, catchment-based rainfall–runoff module that routes water from defined catchments to the MIKE 11 rivers. This module can be used to simulate runoff from mountain catchments that are not included in the MIKE SHE model domain.

2.2. Surface water heat transport modeling

Stream temperature is typically modeled one-dimensionally along the channel longitudinal axis. This is justified by the fact that water temperature in rivers is usually (when there are no point sources) relatively uniform with depth and only small changes are observed in the transverse direction (Cassie, 2006). The conservation of heat in a one-dimensional vertically and laterally well-mixed open channel is described by Gu et al. (1998) as,

$$\frac{\partial T}{\partial t} = \frac{1}{A}\frac{\partial (QT)}{\partial x} + \frac{\partial}{\partial x}\left(D\frac{\partial T}{\partial x}\right) + \frac{H_{ATM} + H_{SED}}{d\rho C_p} \quad (1)$$

where T is the average water temperature in a channel cross-section (°C); Q the flow (m^3/s); A the cross-sectional area (m^2); D the longitudinal dispersion coefficient (m^2/s); H_{ATM} the net rate of heat exchange between water and atmosphere, H_{SED} the net rate of heat exchange between water and sediment bed ($J/s\ m^2$); d the water depth (m); ρ the density of water (kg/m^3); C_p the specific heat of water (J/kg K); t the time (s); and x is the longitudinal distance in the channel (m).

Eq. (1) is analogous to the advection–dispersion equation for the conservation of mass and can be solved using the MIKE 11 Advection–Dispersion (AD) module. MIKE 11 AD solves the one-dimensional advection–dispersion equation numerically using an implicit finite difference scheme (DHI, 2009b). The AD module is dynamically coupled with the Hydrodynamic Module (HD) in MIKE 11, which in turn is dynamically coupled to the MIKE SHE flow model. Thus, flows and temperatures can be modeled simultaneously.

The first two terms of the right hand side of Eq. (1) represent the rate of change of temperature due to advection and dispersion processes. The last term represents heat sources and sinks, which are dependent on numerous processes that vary in space and time (described in the following section). Some of these processes are dependent on hydrodynamic variables (such as discharge, surface area, and water depth) and some are dependent on the calculated water temperature. Thus, the source/sink term is nonlinear and is calculated using a process equation solver called ECO Lab.

ECO Lab calculates the rate of change of any type of state variable given any number of related variables, processes, and forcings (DHI, 2009c). ECO Lab acts as a post-processor of the AD module for every time step. The numerical approach is a split operation scheme where in a given simulation time step, the AD module first transports the temperature solving Eq. (2a), then ECO Lab updates the temperature value by calculating Eq. (2b), which includes all the heat source/sink processes. ECO Lab treats the temperature given by the AD module as a constant, and a new updated value is then used in the next AD time step. ECO Lab does an explicit time-integration of the state variable using either an Euler or

Runge–Kutta integration method. Through testing of the numerical solution against analytical solutions a fixed 1-min time step was determined to be appropriate for the HD and AD calculations (see Appendix A: Runkel, 1996; Lowney, 2000). However, the ECO Lab equations can be calculated at a lower frequency to save computational time. After some testing to ensure the stability of the output, a 30-min time step was chosen for the heat balance calculations in ECO Lab.

$$T_{i+1/2} = \left(\frac{1}{A}\frac{\partial(QT_{i+1})}{\partial x} + \frac{\partial}{\partial x}\left(D\frac{\partial T_{i+1}}{\partial x}\right)\right)\Delta t + T_i \tag{2a}$$

$$T_{i+1} = \left(\frac{H_{net}(T_i)}{d\rho C_p}\right)\Delta t + T_{i+1/2} \tag{2b}$$

where i is the time step and H_{net} is the net heat transfer (J/s m^2) = $H_{ATM} + H_{SED}$ from Eq. (1).

2.3. Heat balance processes

A diagram of the heat balance processes included in the temperature model is shown in Fig. 2. Atmospheric heat fluxes include net shortwave solar radiation (H_S), net atmospheric longwave radiation (H_A), longwave radiation from water (H_{BR}), conductive heat transfer (H_C), and evaporative heat transfer (H_E) (Thomann and Mueller, 1987). The net heat flux between the stream and the sediment bed (H_{GW}) is the sum of conduction and advection. Heat from runoff sources is also included. Each of these processes is described below.

2.3.1. Net solar radiation

Solar radiation is the incoming energy from the sun transmitted through short-wavelength electromagnetic waves. It is considered the most important source of heat into streams (Boyd and Kasper, 2003). The amount of radiation that reaches the water column depends on: (1) the position of the sun, (2) atmospheric scattering and adsorption, (3) reflection, and (4) shading (Chapra, 1997). To estimate the amount of solar radiation that reaches a stream segment, the measured solar radiation is reduced by the reflection from the stream (or albedo) and shading. In order to do this, the global solar radiation must first be separated into the direct beam and diffuse components as the albedo and the shading effects reduce these components differently (Chen et al., 1998). Diffuse solar radiation reaches the stream from all directions through vegetation openings (Boyd and Kasper, 2003). The shading effects on direct beam radiation depend on the topographic and vegetation angles in relation to a stream segment and the stream segment geometry (Chen et al., 1998).

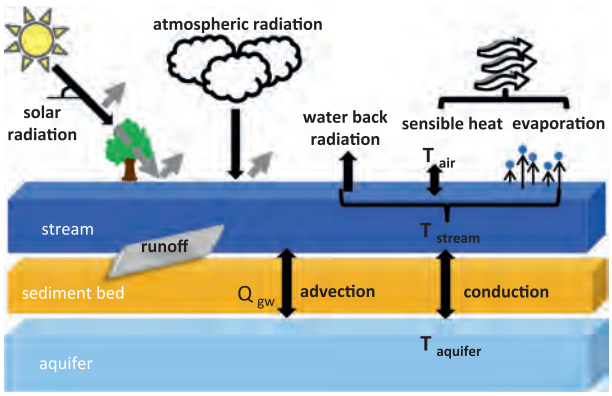

Fig. 2. Conceptual diagram of the heat exchange processes.

Eq. (3) is used to calculate the amount of solar radiation in the model (Chen et al., 1998).

$$H_S = S_f(1 - albedo)H_{dir} + \theta_{vts}0.91H_{diff} \tag{3}$$

where H_S is the net solar radiation (W/m^2); H_{dir} the direct beam solar radiation (measured global solar radiation – measured diffused solar radiation) (W/m^2); H_{diff} the measured diffuse solar radiation (W/m^2); and S_f is the shading factor (–), given by Eq. (4) (Chen et al., 1998); albedo is the surface albedo of the water (–), from Boyd and Kasper (2003); θ_{vts} the sky openness (–), from Chen et al. (1998); and 0.91 = 1 – water reflection of diffuse radiation, assumed to be a constant value of 9% (Sellers, 1965).

$$S_f = 1 - V_{shd}/S_{wid} \tag{4}$$

where V_{shd} is the effective shade width by vegetation (m), which is a function of the position of the sun, stream orientation, vegetation height, density, and distance from stream and S_{wid} is the stream segment width (m). The procedure to calculate S_f was based on Chen et al., 1998.

2.3.2. Net atmospheric radiation

Atmospheric radiation is the energy emitted by Earth objects and atmospheric gasses in the infrared part of the electromagnetic spectrum. Eq. (5) was used in the model to describe atmospheric radiation (Chapra, 1997).

$$H_A = \sigma(T_{air} + 273)^4(aLW + bLW\sqrt{e_{air}})(1 - RL) \tag{5}$$

where H_A is the atmospheric radiation (W/m^2); σ the Stefan–Boltzmann constant (5.67×10^{-8} W/m^2 K^4); T_{air} the temperature of the air (°C); aLW and bLW the empirical constants (–) (Viswanadham and Ramanadham, 1970); e_{air} the air vapor pressure (mbar); and RL is the reflection coefficient (–). Air vapor pressure e_{air} (mbar) is given by the following equation:

$$e_{air} = R_h\left(6.1275 \cdot \exp\left(\frac{17.27T_{air}}{237.3 + T_{air}}\right)\right) \tag{6}$$

where R_h is the relative humidity (%).

2.3.3. Water radiation

Longwave back-radiation from the water is calculated by the following equation:

$$H_{BR} = \epsilon\sigma(T_{sw} + 273)^4 \tag{7}$$

where H_{BR} is the back radiation (W/m^2); ε the emissivity of the water (–); σ the Stefan–Boltzmann constant (5.67×10^{-8} W/m^2 K^4); and T_{sw} is the temperature of the water (°C).

2.3.4. Latent heat flux

Latent heat flux is the amount of energy that is used to convert water from the liquid phase to the gas phase during the evaporation process and it is calculated by the Penman equation (8) (Penman, 1948):

$$H_E = f_{wind} \cdot (e_s - e_{air}) \tag{8}$$

where H_E is the evaporation heat loss (W/m^2); f_{wind} the wind function (W/m^2 mbar); e_{air} is given by (6); and e_s is the saturated water vapor (mbar), calculated by the following equation:

$$e_s = 6.1275 \cdot \exp\left(\frac{17.27T_{sw}}{237.3 + T_{sw}}\right) \tag{9}$$

The wind function is calculated using the following equation (Penman, 1948):

$$f_{wind} = Wa(1 + Wb \cdot U) \tag{10}$$

where f_{wind} is the wind function (MJ/m^2 day kPa); U the wind speed (m/s) measured at 2 m above the surface; and Wa and Wb are the empirical parameters for the wind function (MJ/m^2 day kPa and s/m, respectively).

2.3.5. Sensible heat flux

Sensible heat flux occurs due to the temperature difference between the water and air at the air–water interface. It represents the transfer of heat from molecule to molecule from the temperature gradient (conduction) and by the mass movement of the fluids (convection) (Chapra, 1997). Molecular diffusion is small compared to turbulent diffusion, thus sensible heat transport is mainly caused by turbulent diffusion in the atmospheric surface layer (Arya, 2001). The sensible heat flux is calculated by the following equation:

$$H_c = c1 \cdot f_{wind} \cdot (T_{sw} - T_{air}) \tag{11}$$

where H_c is the sensible heat flux by conduction and convection (W/m^2); $c1$ the Bowen coefficient (mbar/K); f_{wind} the wind function; T_{sw} the temperature of the water (°C); and T_{air} is the temperature of the air (°C).

2.3.6. Groundwater heat flux

Groundwater temperature is not simulated in the model; instead it is an input to the model based on shallow groundwater temperature measurements and it is assumed to be spatially uniform. The following method was developed to simulate surface water–groundwater heat exchanges through a sediment bed from conduction and advection processes.

We use the general equation for groundwater heat flux in the vertical direction (Domenico and Schwartz, 1998) to estimate the heat flux through the sediment bed:

$$H_z = -K_T \frac{\partial T}{\partial z} + qTC_w \tag{12}$$

where H_z is the heat flux in the vertical direction (W/m^2); T the temperature of the upper layer of the aquifer (°C); q the vertical Darcy flow velocity (in the z direction) = fluid velocity × porosity (m/s); K_T the thermal conductivity of the bulk streambed sediments (W/m K); C_w the heat capacity of water (J/m^3 K); and z is the depth (m). The first term of the right side of the equation describes the heat flux by conduction (Fourier's Law), which depends of the thermal gradient. The second term describes the heat flux by advection, which depends on the groundwater flow velocity.

In order to solve for H_z in Eq. (12) and find $\frac{\partial T}{\partial z}$ and T, we solve the steady state one-dimensional groundwater heat transport equation given by the following equation (Bredehoeft and Papadopulos, 1965):

$$K_T \frac{\partial^2 T}{\partial z^2} - qC_w \frac{\partial T}{\partial z} = 0 \tag{13}$$

where T is the temperature of the upper layer of the aquifer (°C); q the groundwater flux (m/s); K_T the thermal conductivity of the bulk streambed sediments (W/m K); C_w the heat capacity for water (water density × specific heat) (J/m^3 K); z the depth (m); and t is the time (s). The solution of Eq. (13) under steady state conditions was derived by Bredehoeft and Papadopulos (1965) for boundary conditions $T = T_{sw}$ at $z = 0$ and $T = T_a$ at $z = L$.

$$\frac{(T - T_{sw})}{(T_a - T_{sw})} = \frac{[\exp(\frac{\beta z}{L}) - 1]}{[\exp(\beta) - 1]} \tag{14}$$

where T is the temperature at depth z below the stream (°C); L the length of the sediment bed; T_{sw} the temperature at the top of aquifer (assumed to be the stream temperature); T_a the temperature of the aquifer (assumed to be constant below depth L); $\beta = C_w qL/K_T$ (–); and z is the depth (positive downward).

Using Eq. (14) we can solve for T, take the derivative dT/dz, and substitute into Eq. (12) given that we know T_{sw} (stream temperature) and T_a (aquifer temperature). The resulting groundwater heat flux Eq. (15) is:

$$H_{GW} = qC_w \left[\left(\frac{(T_{sw} - T_a)}{\exp(\frac{C_w qL}{K_T}) - 1} \right) + T_{sw} \right] \tag{15}$$

where T_{sw} is the stream temperature and T_a is the aquifer temperature.

The validity of the steady state assumption was tested against a transient numerical model (see Appendix B). The test shows that errors are significant during periods of low heat flux and low during periods of higher heat flux. The performance of the steady-state approximation is therefore appropriate for this regional-scale study.

2.3.7. Drainage heat flux

There are few studies that deal with the heat contribution of agricultural runoff, but it has been shown that water temperature in agricultural fields can be much higher than in nearby streams (Fujimoto et al., 2008). Heat flux from agriculture is estimated by Eq. (16) assuming that the field temperatures are in equilibrium with the atmosphere. The equilibrium temperature is the water temperature at which the sum of all heat fluxes is zero (Bogan et al., 2003). The water equilibrium temperature was calculated using the time series climate data to calculate the atmospheric heat balance terms: H_S, H_A, H_{BR}, H_C, and H_E. Since the last three terms are water temperature dependent and the equation is nonlinear, a Newton–Raphson numerical method (Chapra and Canale, 1998) was used to solve for the water temperature. For solar radiation, the measured global radiation data was used. The equilibrium temperature was calculated at an hourly time step and then averaged to daily time steps because the hourly calculation is likely to be more dynamic than the water temperature due to the thermal inertia of the water (Bogan et al., 2003). Heat input from agricultural runoff was then computed with the following equation:

$$H_d = Q_d T_{eq} \frac{\rho C_p}{A} \tag{16}$$

where H_d is the heat flux from agricultural runoff (W/m^2); Q_d the drainage flow, calculated by MIKE SHE (m^3/s); T_{eq} the equilibrium temperature (K); ρ the density of water (kg/m^3); C_p the specific heat of water (J/kg K); and A is the surface area of the stream segment (m^2).

3. Study site description

Silver Creek is a spring-fed system abundant in wildlife and an important trout habitat in the United States (Wetzstein et al., 2000). Intensive water use and land use management have contributed to lower flows and increased sediment loads and temperatures, which are threatening the aquatic ecology of Silver Creek (Gillilan, 2007; Ecosystem Sciences Foundation, 2011). Silver Creek is located in south-central Idaho and is part of the Snake River Basin (Fig. 3). The source of water to Silver Creek is an alluvial aquifer that links two surface water basins, the Big Wood River Basin (BWRB) and the Little Wood River Basin. Silver Creek is a tributary of the Little Wood River, but the Big Wood River (BWR) and its diversion canals recharge the aquifer that feeds the Silver Creek Basin (SCB). The Big Wood River-Silver Creek aquifer system underlies a triangular valley, the Wood River Valley, surrounded by mountains on all sides. These are part of the Rocky Mountains and have elevations up to 4000 meters above mean sea level

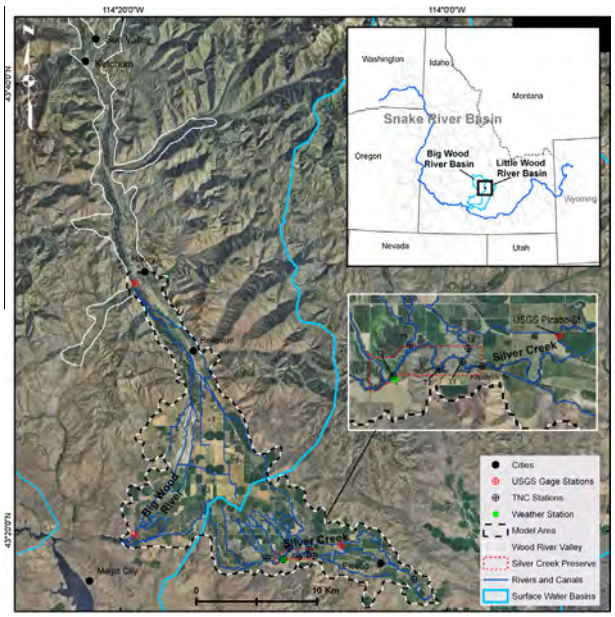

Fig. 3. Study area, Wood River Valley and Silver Creek Basin.

(mamsl). Several mountain canyons are the source of water to the BWR, which flows towards the southwest part of the Wood River Valley. Silver Creek is formed by springs in the south-central part of the valley and exits the valley at the southeast corner.

This study focuses on the Lower Wood River Valley, south of the city of Hailey. It is an area of approximately 231 km^2 with elevations ranging from 1400 to 1700 mamsl. The northern boundary of the study area was chosen to coincide with the location of a USGS flow gage on the BWR with long-term continuous measurements. Flow to the BWR comes from 25 tributary canyons, most of which are located north of the study area (Bartolino, 2009). These tributaries can be perennial or ephemeral, but most streams flow only in response to precipitation or snowmelt, and some water reaches the BWR by subsurface flow (Bartolino, 2009).

Surface and subsurface flows from the northern BWRB enter the lower valley at Hailey; some of the BWR flow is diverted by a system of irrigation canals, some is lost to the aquifer system by seepage, and the rest leaves the valley in the southwest corner.

The Wood River Valley aquifer system includes unconfined and confined aquifers comprised primarily of the fluvial and glacial sediments of the Quaternary period (Skinner et al., 2007). The valley is filled to depths of as much as 150 m with a sequence of interbedded clay, silt, sand, and gravel (Moreland, 1977). Groundwater flow is unconfined in the northern areas of the valley. The transmissivity decreases towards the south due to fine sediment layers beginning at the center of the valley and increasing in thickness to the south forming a confining unit. The groundwater flow direction is split into the southeast and southwest areas of the valley where some of it discharges as springs. In the southeast corner, the Snake River Basalt forms a deep unconfined aquifer with high transmissivities.

Springs are formed in the central area of the valley where the confining units constrain the movement of groundwater. Some of these springs flow to the west into the Big Wood River and some form the tributaries that flow southeast to Silver Creek. Spring flow increases in August through November then decreases through the winter (Brockway and Kahlown, 1994). The average flow in Silver Creek is around 4 m^3/s. Maximum flow occurs in March or April due to local snowmelt runoff from surrounding mountains (around 10–12 m^3/s) and minimum flow occurs in the summer (around 1.2–2 m^3/s) (US Geological Survey, 2010a).

The climate of the Lower Wood River Valley is semi-arid with low precipitation and high evapotranspiration (Brockway and Kahlown, 1994). The total annual precipitation is 310–420 mm, with 60% falling during winter, mostly as snow (Bartolino, 2009). The coldest and wettest month is January, with average temperatures ranging from −5.8 °C in the southern valley to −6.8 °C at Hailey; the warmest is July (20 °C in the south to 19 °C at Hailey) (Skinner et al., 2007).

The valley is intensely cultivated (around 60% of the area) and approximately 80% of the crops area is irrigated (Brockway and Kahlown, 1994). The growing season typically occurs from May to September. Approximately half of the irrigation water comes from diversion canals and half from groundwater pumping. Water for agriculture is also diverted from the spring-fed creeks and canals in the south. The canals and ditches carrying water to the fields significantly contribute to aquifer recharge (Brockway and Kahlown, 1994).

There have been several groundwater studies of the Wood River Valley (Moreland, 1977; Brockway and Grover, 1978; Wetzstein et al., 2000; Bartolino, 2009), but none of the studies have focused on the river hydrology and its implications for ecological status. An integrated surface water–groundwater model of the Wood River Valley is able to provide this type of information.

4. Model application

Silver Creek flow cannot be properly simulated without including the BWR dynamics in the lower valley, diversions and seepage from the irrigation canals, and groundwater flow in the valley. In order to maximize computational efficiency, the modeling was performed at two scales: (1) a larger area that includes the entire Lower Wood River Valley, outlined in black in Fig. 3 and (2) a smaller area that only includes the SCB (of which the northern boundary is the BWRB-SCB surface water divide outlined in blue in Fig. 3). The flow model was calibrated for the larger area. However, coupling the temperature model to the flow model increases the computational time by a factor of 2–3, and modeling the temperature in the BWRB was not considered necessary; thus, the temperature model was applied only to the SCB. The groundwater flow along the BWRB–SCB basin divide was extracted from the larger model and used as a groundwater flux boundary condition for the SCB model.

4.1. Flow model inputs

The model was built using a cell size of 300 m. The cell size was chosen after a trial and error process, trading off computational time, stability of the surface water–groundwater exchange, and representation of spatial details of the landscape. The model inputs and the data sources are listed below. The time steps for the flow time series data inputs were hourly or daily.

1. *Precipitation and snow*: Daily precipitation and hourly air temperature time series for the simulation period were obtained from the AgriMet database (US Bureau of Reclamation, 2010). To calculate snowmelt the degree-day factor used is 2 mm °C^{-1} d^{-1} and the melting temperature was set at 0 °C.
2. *UZ–ET*: ET Idaho, 2010: Daily time series of reference evapotranspiration were also obtained from the AgriMet database. A land use/vegetation map was obtained from the National Land Cover Dataset (US Geological Survey, 2010b). A total of 16 land use/vegetation types were included in the model. Time series for the vegetation parameters required for the actual ET calculation (crop coefficients, root depths, LAI) were created based on vegetation and crop cycles from Allen et al. (1998). The crop

cycles were assumed to be the same for every year of the simulation. A soil map and soil parameters for each soil type (the moisture contents at saturation, at field capacity, at wilting point and the maximum infiltration rates) were obtained from the Natural Resource Conservation Service Soil Survey database for Blaine County, Idaho (US Department of Agriculture, 2010). A total of 58 soil types were included in the model.

3. *SZ*: The geologic model consists of three layers: the unconfined aquifer, the confining unit, and the confined aquifer. The thickness of these layers is spatially defined based on borehole data from the Well Drillers Reports (Idaho Department of Water Resources, 2010). Due to the complexity of the hydrogeologic layers in the model area, several geologic interpolation iterations were used during the calibration process. The hydraulic conductivities for the geologic layers were also varied during the calibration. The groundwater boundaries are the estimated subsurface flow at the north following a procedure used by Bartolino, 2009, a fixed head boundary at the southeast corner using measured groundwater elevations, and a zero-flow boundary around the rest of the model boundary.
4. *Drainage*: Agricultural fields are drained by a system of ditches that route the water to canals, streams, and recharge ponds. Agricultural runoff is simulated by the drainage module and was specified for all the crop cells of the model.
5. *Irrigation*: Irrigation areas, which correspond to the crop cells in the model, were grouped according to the source canal that supplies water to specific areas in the valley. The measured flows by the Irrigation District 37 Water Master (Water District 37 and 37-M, 1999) were used to specify the amount of water diverted to the irrigation canals. Some of this diverted water is lost by seepage to the aquifer; thus, surface water diversions do not satisfy all of the irrigation demand. Since time series data of groundwater abstractions are not available, the groundwater irrigation setup in the model simply supplies the necessary water when water is not available in the canals. Irrigation demand was specified based on calculated crop evapotranspiration requirements for each crop type.
6. *Surfacewater*: The main inputs for the surface water model are a map of the rivers and canals and cross-sectional data. The river center lines were based on data from the National Hydrography Dataset (US Geological Survey, 2010c) and aerial photography. Cross-sectional data were obtained mainly from a cross-section survey conducted by The Nature Conservancy in 2010 and aerial photography. Operating gates and pumps in MIKE 11 were used to control the irrigation diversions.
7. *Rainfall–Runoff*: The measured flow at Hailey (US Geological Survey, 2010b) was specified at the northern surface water boundary. The flow at this location comprises most of the mountain runoff to the BWR. To simulate runoff from the mountain basins in the southern valley, the NAM model was linked to the surface water model. The mountain catchments were delineated using the StreamStats web tool (US Geological Survey, 2010d).

4.2. Temperature model inputs

Time series data were entered as forcings for the heat balance equations. These data were obtained from the Picabo weather station located approximately 150 m south of Silver Creek at an elevation of 1494 mamsl (US Bureau of Reclamation, 2010). The following hourly time series were inputs to atmospheric heat exchange module:

- Global solar radiation.
- Diffuse solar radiation.
- Air temperature.
- Relative humidity.
- Wind speed.

The stream orientation was calculated for all the streams in the model using the TTools routines for ArcGIS (Boyd and Kasper, 2003), using a stream segment discretization of 500 m. The vegetation parameters (height, width, and density) needed for shading calculations (Eq. (4)) were estimated using the land cover map. For this case, the topographic shade angles were neglected since the topography near the streams is relatively flat. Other constant parameters for the heat balance equations were obtained from literature sources or model calibration (Appendix C). (Appendix C: TNC, 2011; Hill, 1998).

Continuous groundwater measurements taken for 1 year as part of this study show that deep groundwater temperature is fairly constant throughout the year, but also that there is a seasonal variability in shallow groundwater temperature ($\sim$1 m from the surface). Since shallow groundwater interacts directly with surface water, a time series of groundwater temperature was generated based on the 1-year measurement of shallow groundwater.

There are no temperature boundaries specified in the temperature model, except for the calculated equilibrium temperature which is specified for the runoff flow and the groundwater temperature linked to the groundwater flow. Thus, the temperature model is completely driven by the transport and heat balance processes described above.

4.3. Model calibration

In order to evaluate the model performance under different climate conditions, the flow model was calibrated for the period 2003–2009. In terms of the ecological implications, the periods of greater concern are during low flow and high temperatures in Silver Creek. Thus, the calibration of the flow model was mostly focused on minimizing the error in the Silver Creek flow, specially the low summer flow. Nevertheless, accuracy of the flow volumes in the BWR, the Silver Creek tributaries, and of groundwater elevations were also taken into account as part of the calibration process.

The main objective of the calibration was that the distribution of water in the valley is properly represented. That is, the irrigation application, crop evapotranspiration, canal seepage, and spring discharge should be within a reasonable volume range compared to the data available and to previous studies of the area. Some work was also invested in reducing potential sources of numerical errors that occur in the dynamics of surface water–groundwater exchange. For example, ensuring consistency in the interpolated topography of MIKE SHE and the more detailed topography in MIKE 11. Interpolation of the geology is another critical part of the model. The depth of the confining unit in the southern part of the valley has a significant impact on both groundwater levels and Silver Creek flow. Because of the complexity of the geology, the interpolation into the three groundwater model layers can vary greatly and it should be carefully interpreted. During the calibration process, the borehole data were carefully examined, compared to previous geologic studies of the valley, and re-interpolated several times. Finally, a set of semi-automatic calibration runs was performed varying hydraulic conductivities and leakage coefficients.

A sensitivity analysis and calibration of the atmospheric heat balance parameters and the stream roughness coefficient were performed for a surface water model of Silver Creek using the measured flow and temperature of the tributaries as boundary conditions (Appendix C: Hill, 1998). The final values used for the flow and temperature model parameters are shown in Table 1.

The Nature Conservancy (TNC) owns and manages a preserve that includes approximately 4 km of Silver Creek and some portions of its tributaries (Fig. 3). TNC has measured flow and

temperature in five locations (T1–T5 in Fig. 3) during the summer months since 2005. In addition, there is a gage station operated by the USGS that measures water levels and temperature every 15 min. The USGS converts water level measurements to flow by using rating curves (Kennedy, 1984). The stability of the rating curve is checked by taking flow measurements in the field at variable frequencies that can range from weeks to months, but it is usually done on a monthly basis (US Geological Survey, 2010a).

The statistics used to compare the model results against observed data during the calibration process were the mean error (*ME*), and root mean square error (*RMSE*), and the correlation coefficient (*R*) (DHI, 2009a).

$$ME = \frac{\sum_t (Obs_{i,t} - Calc_{i,t})}{n} \tag{18}$$

$$RMSE = \frac{\sum_t \sqrt{(Obs_{i,t} - Calc_{i,t})^2}}{n} \tag{19}$$

$$R = \frac{\sum_t \left(Calc_{i,t} - \overline{Calc}_{i,t}\right) \times \left(Obs_{i,t} - \overline{Obs}_{i,t}\right)}{\sqrt{\sum_t \left(Calc_{i,t} - \overline{Calc}_{i,t}\right)^2 \times \sum_t (Obs_{i,t} - \overline{Obs}_{i,t})^2}} \tag{20}$$

5. Results

5.1. Calibration

The flow calibration statistics for the simulation period (2003–2009) at the Silver Creek and BWR USGS gage stations are shown in Table 2. The Silver Creek station is located downstream of the tributaries and major points of diversions (Fig. 3) and the BWR station is located at the southwest outlet of the model area. The BWR flow matches the observed data quite accurately, which means that the volume of water taken out by seepage losses and diversions in the river is well represented. The simulated flow in Silver Creek at the USGS station follows the trends of the measured flow most of the time. The largest errors occur during the spring high flow periods, during which the model underestimates the peaks.

Table 2
Flow calibration statistics.

Location	ME (m^3/s)	RMSE (m^3/s)	R (–)
Silver Creek	−0.13	0.71	0.78
BWR	−0.95	2.78	0.99

The distribution of tributary flows in the SCB is particularly important for the temperature model because the different conditions of the tributaries can lead to different temperatures in Silver Creek. For example, tributaries may be exposed to different amounts of shading, have different flow regimes and receive flow from different sources (groundwater vs. agricultural runoff). A comparison of the flow distribution calculated from measured data vs. that predicted by the model is shown in Table 3. According to model results, 48% of the Silver Creek flow comes from Grove Creek and 52% comes from Stalker Creek and Loving Creek; the measured flow indicates that 44% comes from Grove Creek and 56% of the flow comes from Stalker Creek and Loving Creek. As discussed further below, this difference could potentially lead to colder simulated temperatures in Silver Creek because Grove Creek is a colder system than both Stalker Creek and Loving Creek.

The simulation period for the temperature model is shorter than that for the flow model (April 2007–September 2009) because of the availability of some of the model input and calibration data. In general, the simulated temperature matches the trends of the measured temperature at the USGS Picabo station (Fig. 4). The mean error for the period of 2007–2009 is 1.1 °C, the RMSE is 1.7 °C, and the correlation coefficient is 0.98. The high correlation coefficient indicates that the dynamics are well represented, i.e., the timing of the peaks and lows matches very closely with the measured data. The simulated temperature error is smaller during periods when simulated flow errors are smaller, such as in the summer months of 2008 (Fig. 5).

5.2. Groundwater flow and stream temperature

According to the simulated water balance, the flow through the BWRB–SCB divide accounts for 79% of the SCB inflow, the rest

Table 1
Model parameters.

Model component	Parameter symbol[a]	Calibrated[b]	Final value (unit)
Solar radiation	Albedo	No	Time varying[c] (–)
Atmospheric radiation	Empirical constant (*aLW*)	Yes	0.7 (–)
Atmospheric radiation	Empirical constant (*bLW*)	Yes	0.065 (–)
Atmospheric radiation	Reflection coefficient (RL)	Yes	0.03 (–)
Water back radiation	Emissivity of water (ε)	Yes	0.95 (–)
Atmospheric/water back rad.	Stefan–Boltzmann constant (σ)	No	5.67×10^{-8} ($W/m^2\ K^4$)
Evaporation/sensible heat	Wind function constant (*Wa*)	Yes	6.43 ($MJ/m^2/day/kPa$)
Evaporation/sensible heat	Wind function constant (*Wb*)	Yes	0.536 (s/m)
Sensible heat	Bowen coefficient (*c*1)	Yes	0.63 (mbar/K)
Groundwater heat	Thermal conductivity (K_T)	No	1.65 (W/m/°C)
Groundwater heat	Sediment bed depth (L)	No	1 (m)
Heat flux term	Water density (ρ)	No	998 (kg/m^3)
Heat flux term	Specific heat of water (C_p)	No	4182 (J/kg/°C)
Surface water heat transport	Dispersion coefficient (D)	Yes	10 (m^2/s)
Surface water flow	Manning's (n)	Yes	0.09 ($s/m^{1/3}$)
Sw–gw flow exchange	Leakage coefficient	Yes	1×10^{-6}–1×10^{-5} (1/s)
Groundwater flow	Kh[d] L1	Yes	0.001–0.03 (m/s)
Groundwater flow	Kh L2	Yes	1×10^{-8} (m/s)
Groundwater flow	Kh L3	No	0.001 (m/s)
Agricultural runoff	Drainage time constant	No	1×10^{-7} (1/s)

[a] Refer to Eqs. (1), (2a), (2b), (3)–(15).
[b] Initial values and non-calibrated values obtained from various literature sources.
[c] Time varying based on solar zenith angle.
[d] Horizontal hydraulic conductivities for groundwater model layers L1 (unconfined aquifer), L2 (confining unit), and L3 (confined aquifer). The vertical hydraulic conductivities are the same as the horizontal except for L3 which is a factor of 10 less than the horizontal conductivity (0.0001 m/s).

Table 3
Average contribution of tributaries to Silver Creek flow.[a]

Tributary	Simulated flow (%)	Measured flow (%)
Stalker Creek[b]	37	34
Grove Creek	48	44
Loving Creek	15	22

[a] Flow simulated at the USGS Picabo station.
[b] Includes Buhler Drain, Patton Creek, Chaney Creek, and Mud Creek.

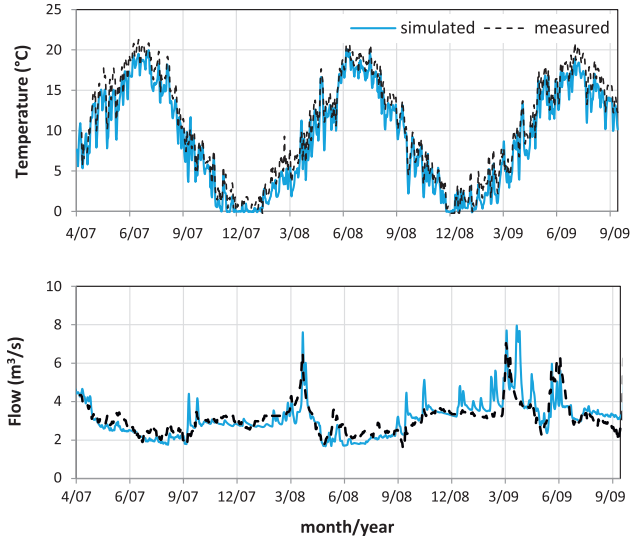

Fig. 4. Simulated vs. measured average daily stream temperature and flow in Silver Creek (at USGS Picabo St.).

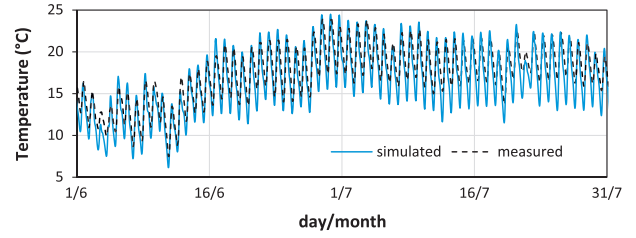

Fig. 5. Simulated vs. measured hourly stream temperature in Silver Creek during the summer of 2008 (at USGS Picabo St.).

comes from mountain catchments and precipitation. There is no direct surface water connection between the BWRB and the SCB; all of the inflow to the SCB from the BWRB is through groundwater flow. This groundwater flow comes to the surface water as springs in the north of the basin which feed the Silver Creek tributaries. Currently, about 25% of the inflow to the valley is used for irrigation. As the water demand for irrigation increases in combination with increasing urban developments, the system is becoming increasingly stressed which results in higher potential impacts to the ecology of Silver Creek. The relationship between groundwater flow across the BWR and SCB divide and the stream temperature in Silver Creek was tested by reducing this flow by 10% four times. Each simulation was run for a period of 3 years. Fig. 6 shows the change in average and maximum stream temperatures as a result of reducing the groundwater flow. Each 10% reduction caused on average a 0.3 m^3/s reduction in the Silver Creek flow, which causes a 0.3 °C increase in the average temperatures from late spring to early fall (May–September) and 1.5 °C increase in the maximum temperatures.

5.3. Spatial distribution of solar radiation

As previously mentioned, solar radiation is the most important atmospheric heat input during most of the year. The amount of solar radiation varies in space and time due to several factors discussed above. Although the spatial variation of solar radiation changes during the day, in areas that are well shaded solar radiation remains consistently lower than areas without shade. During the peak hours of the warmest day of the simulation period solar radiation varies from less than 100 to over 900 W/m^2 (Fig. 7) and the cumulative daily solar heat input varies from 7 MJ/m^2 to 646 MJ/m^2.

The shading potential not only depends on the type of stream vegetation, but also on the width of the stream. Even if the same type of vegetation was specified for all locations in the model, there would still be a spatial variation of solar radiation throughout the basin, mainly due to stream geometry; i.e., the potential shading effect is higher at narrower cross-sections.

5.4. Spatial distribution of heat sources and temperature

The spatial distribution of temperature in the streams is mostly a function of the flow volume, the flow source, and the amount of solar radiation. The fraction of the total heat input for each of the incoming heat components for each of the Silver Creek tributaries was calculated for each day for the year 2008 (Fig. 8). The incoming heat components are: solar, atmospheric, groundwater, and drainage runoff. For the calculation of total atmospheric heat input, the sensible heat was added to the atmospheric heat at the times when it is a heat gain to the stream (i.e., when the temperature of the air is higher than the water temperature). Fig. 8 also shows the percentage of the total flow each tributary contributes to the total flow in Silver Creek and the daily average temperature in the stream. The results reveal that in addition to the volume of flow, the source of heat and flow determines the stream temperature signal. Buhler Drain and Patton Creek have high summer temperatures (>20 °C) due to low flow volume, mostly from agricultural runoff, and high solar radiation. Thompson Creek also has low flow volume (2% contribution), but the flow is almost exclusively spring-fed, thus the temperatures are much lower and have low seasonal variations. Moreover, all the streams for which groundwater heat is a larger fraction of the heat input, have much lower and stable temperatures (Cain, Grove, Thompson, and Wilson creeks). Chaney Creek and Mud Creek have similar heat source fractions, but Chaney Creek has a lower flow volume; thus, it has higher temperatures due to lower thermal capacity. Finally, Love Creek has the second largest flow, but most of it is fed by drainage runoff; thus, it has high temperatures and a large seasonal variation.

The average heat input per unit volume for the Silver Creek flow sources was calculated for each month of 2008 (Fig. 9). The values (in units of mega-joules/m^3) were calculated using the following equation:

$$\frac{H}{Q} = \rho C_p T \tag{21}$$

where Q is the flow from the tributary to Silver Creek and T is the water temperature at the mouth of the tributary. From the heat balance equation ($QT = Q_1T_1 + Q_2T_2 + \cdots + Q_nT_n$), flow input with lower temperatures than that of the receiving body will lower the temperature of the stream. Grove Creek has the highest heat input because it contributes the largest amount of flow. However, the heat contribution per volume is greatest from agriculture runoff and lowest from Grove Creek in the summer months because the runoff temperature is assumed to be in equilibrium with the atmosphere,

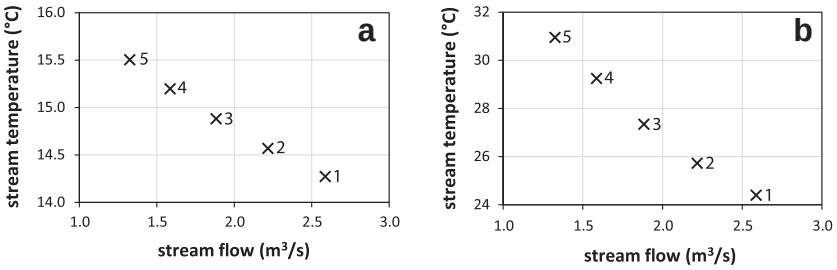

Fig. 6. Stream flow and temperature resulting from decreasing groundwater flow from the BWR to the SCB. Plot a – average stream temperatures during the months of May–September. Plot b – maximum stream temperatures. *x*1 = calibrated groundwater flow; *x*2 = gw1-10% of gw1; *x*3 = gw2-10%gw2; *x*4 = gw3-10%gw3; *x*5 = gw4-10%gw4.

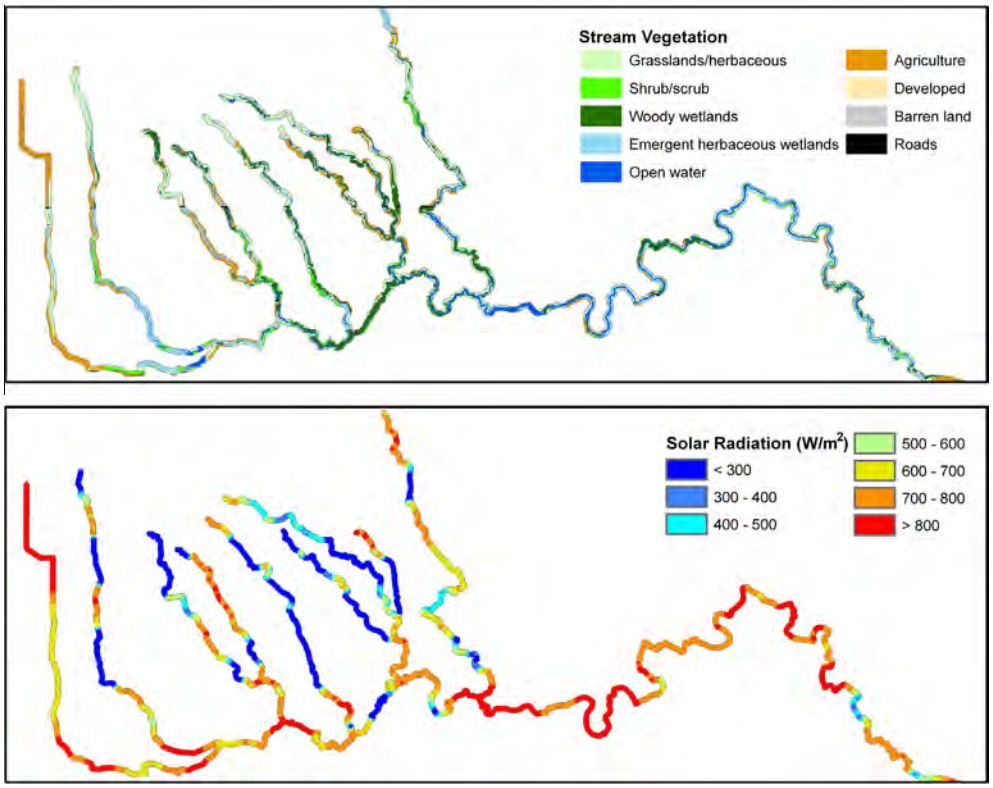

Fig. 7. Stream vegetation and simulated solar radiation on 29 June 2008.

whereas Grove Creek is a spring fed system and its temperatures are closer to the colder groundwater temperatures.

Fig. 10 shows the simulated temperatures for all the streams in the SCB for the hour of the warmest water temperatures in Silver Creek (June 29th, 2008 16:00). Buhler Drain and Stalker Creek are the warmest tributaries. Patton Creek and Cain Creek are colder tributaries but contribute relatively less flow to Stalker Creek. Grove Creek with large spring flows reduces the temperatures and the large diurnal oscillations observed at Stalker Creek at the headwaters of Silver Creek. Loving Creek gets warmer as it flows toward Silver Creek possibly because of the irrigation diversions by the Gillihan Ditch and higher exposure to solar radiation. The downstream areas of Silver Creek also get warmer due to irrigation diversions and some large open water areas (Fig. 7).

6. Discussion

The BWRB contributes 79% of the inflow to the SCB, solely through the aquifer system. The contribution to the groundwater flow comes from river and canal seepage and regional groundwater flow. Thus, it is necessary to understand the hydrology of the Wood River Valley to be able to simulate the flow and temperature of Silver Creek. Furthermore, the water management of the BWRB has a large influence on the habitat conditions in the SCB.

The flow model calibration involved improvements to the distribution of the water balance components in the valley, minimizing numerical errors, and optimizing surface water and groundwater parameters. The calibration statistics for a 7-year period (2003–2009) result in a mean error of 0.13 m^3/s and a correlation coefficient of 0.78 in the flow at Silver Creek. The average percent difference between simulated and measured flows during that time period is 15%. However, flow measurements errors could be up to 20% under certain conditions (Saucer and Meyer, 1992). Water balance components have been compared to the available data from other studies and are within reasonable ranges (Bartolino, 2009; Wetzstein et al., 2000).

In general, the flow model produces fairly reasonable results and is a suitable tool for water management scenarios at the catchment scale. However, given the complexity of the model, there are

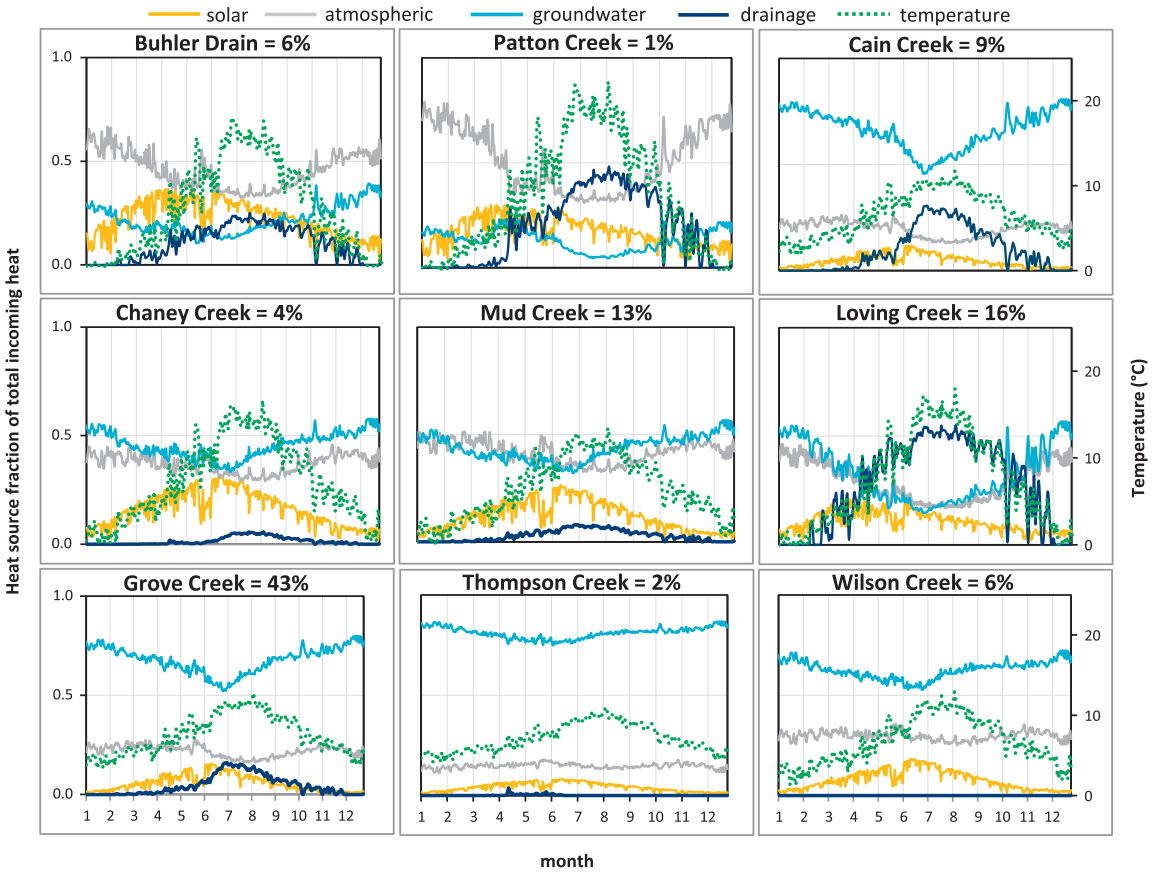

Fig. 8. Simulated fraction of heat sources, temperature, and flow contribution in 2008.

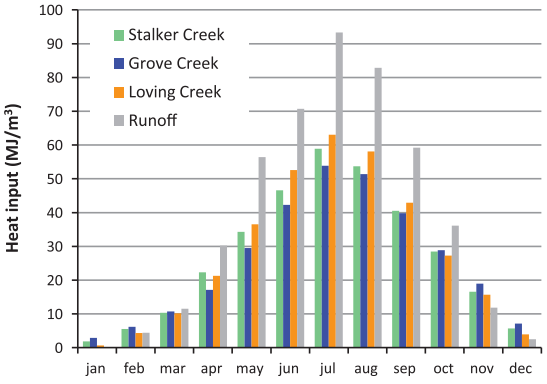

Fig. 9. Monthly average heat input to Silver Creek from flow sources.

some limitations in the input data, the model setup, and the calibration. Some of the areas in which the model could be improved are discussed below:

- Water diversions and abstractions are important components of the water balance. The volume and spatial distribution of water use has been simplified due to a lack of more detailed data.
- The distribution of flow in the tributaries could be adjusted by further calibration of the leakage coefficients and by adjusting the rate and distribution of agricultural runoff. The tributaries are formed as springs, thus further knowledge of the geology and calibration of the groundwater model would also impact the flows in the tributaries.
- Spring runoff flow from mountain catchments tends to be overestimated by the model. Large spring cold-water flow is the likely cause of the low simulated temperatures in the spring. The rainfall–runoff model that was used to generate mountain runoff uses the only weather station available for the model area, which is located in the southern valley. The air temperature measured at the valley is expected to be somewhat higher than the air temperature in the mountains; this could cause earlier snow melt than in reality. Correction of the temperature data for higher elevations should be applied for the rainfall–runoff model.
- Potential errors in the geometry of the stream can lead to under- or over-estimated diurnal variations. Thus, more cross-sectional data are important to improve the temperature model.
- Explicitly modeling the groundwater temperature could improve the accuracy of the heat exchange between the surface water and groundwater. For example, we assume that the groundwater temperature is spatially uniform, but it could potentially be influenced by the surface water temperature.

The calibration statistics for the temperature model result in a mean error for the hourly data for the period of 2007–2009 of 1.4 °C, the RMSE is 1.7 °C, and the R is 0.98 at Silver Creek.

The simulation periods with the lowest flow error tend to show the best performance in the temperature model. However, other sources of errors are the heat fluxes, stream geometry, flow distribution in the tributaries, and/or numerical errors. From the numerical testing (Appendix A), numerical errors could be more than 0.5 °C in areas of the model where the grid spacing is close to the maximum dx set for the model (500 m). At the basin scale, these errors may cancel out and be negligible. However, some grid

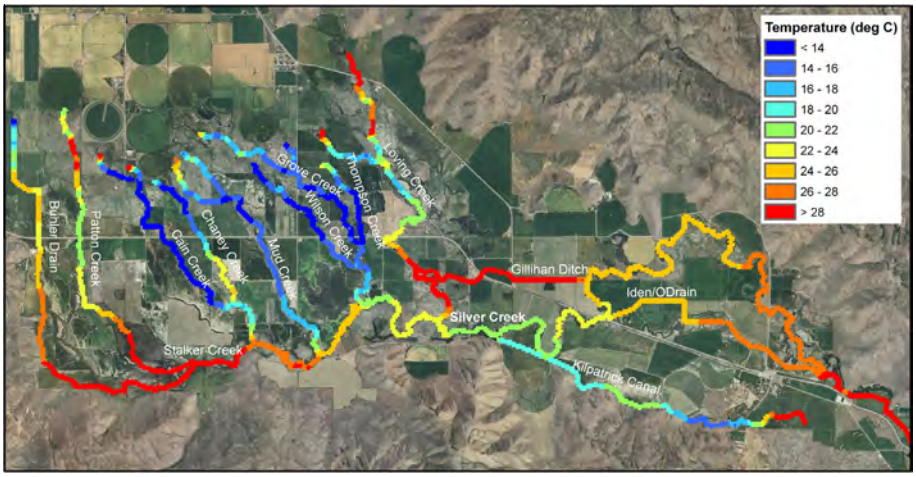

Fig. 10. Simulated stream temperatures at the hour of warmest water temperatures in the downstream portions of Silver Creek (June 29th, 2008 16:00).

refinement may be required in future applications of the model, particularly in areas of high gradient and flow variability.

The hourly stream temperature plot (Fig. 5) shows some over-estimation of the diurnal temperature variation, which may be caused by errors in the geometry of the stream. As previously mentioned, water depth and surface area affect the thermal inertia (the ability to conduct and store heat) and hence, the diurnal amplitude. However, it is also possible that the assumption of complete mixing in the stream in a cross-section fails in some areas of the model. The simulated temperature represents a cross-section averaged temperature, while the temperature data are taken at a certain depth. If there is incomplete mixing in a given stream cross-section, this would not be captured by the model.

The model results show that a reduction of the groundwater flow to the Silver Creek Basin of 10% can cause average and maximum temperature increases of approximately 0.3 °C and 1.5 °C, respectively, in Silver Creek.

The local distribution of groundwater flow and agricultural runoff in the SCB among the tributaries has a strong influence on the Silver Creek flow and temperature. The relative contribution of each tributary system is an essential part of the temperature model and thus, inaccuracies in tributary flows could be a potential source of the temperature error. In the model, Silver Creek receives most of the flow from the colder Grove Creek system, as opposed to the much warmer systems of Stalker Creek or Loving Creek. The average measured temperatures for lower Stalker Creek, Grove Creek, and Loving Creek for mid-June to end of August 2009 are 16, 13, and 17 °C, respectively. While temperature measurements in Grove Creek indicate that it is in fact a colder system than Stalker Creek and Loving Creek, the model is predicting colder temperatures and higher flow in Grove Creek than observed. Reducing the simulated flow in Grove Creek to match the measured data would increase the temperature in this system that contributes half the flow to Silver Creek, and thus potentially reduce the temperature error in Silver Creek substantially. Further flow model calibration with more focus on these three systems (in particular, the surface water–groundwater exchange leakage coefficients and drainage rates) could be the key to improve the temperature results downstream.

There is a large spatial variability of surface water temperature throughout the SCB. During the summer peak hours, temperature spatial variations reach around 15 °C (Fig. 10). This result is valuable for understanding the distribution of ecological conditions in the basin and establishing management priorities. From Fig. 7 it is evident that there are portions along some of the tributaries and Silver Creek with low vegetation buffers that receive a large amount of solar radiation. Thus, there is the potential for riparian vegetation restoration in many areas along the basin. However, the width of the stream segments and, to a lesser extent, the stream orientation in relation to the solar path affects the capability to receive shade from the vegetation. Thus, these factors should be evaluated in stream restoration planning using riparian vegetation.

The spatial distribution of diffuse thermal loads can vary substantially throughout the basin. When climate conditions are fairly uniform, as in this case study, the amount of solar radiation and flow sources and volumes are the main factors that contribute to the thermal load in the tributaries. The impact of the thermal load downstream depends on the relative flow contribution. This concept agrees with other studies that have found the importance of lateral inflow (Westhoff et al., 2007) and groundwater flow contributions (Bogan et al., 2003) in stream temperature models. Water and land management affects the contribution of the diffuse heat sources. For the critical summer months of low flow and high temperatures, increased groundwater use leads to lower input of colder groundwater and increased irrigation leads to higher runoff with potentially warmer flow. Riparian vegetation changes the shading capability, while geomorphology affects the capacity to exchange heat with the atmosphere. The purpose of the model we have developed is to quantify the impact of such scenarios in the stream ecosystem.

7. Conclusions

We have developed a simulation tool that relates how land use and water use affects the temperature distribution in a catchment. The field of ecohydrology seeks to relate hydrology and biota at the catchment scale. As one of the main drivers of aquatic ecology, temperature is a key variable in this context.

A catchment-scale integrated surface water–groundwater flow and temperature model was developed and calibrated. An integrated approach is necessary to fully understand and accurately simulate changes in stream temperatures in Silver Creek because of the strong relationship between groundwater flow and stream temperatures which is clearly reflected in the model results. Moreover, the local conditions in each of the Silver Creek tributaries and the distribution of the flow among these tributaries have a great influence on the flow and temperature in Silver Creek. A combination of solar radiation, flow volumes, and the source of flow

influences the temperatures of the tributaries and thus, the temperature of Silver Creek. Therefore, restoration efforts for Silver Creek have to be evaluated at the catchment-scale and prioritized according to the relative contribution from the tributaries.

Solar radiation is the most important component of the atmospheric heat balance and one that could be significantly altered by catchment management. The spatial distribution of solar radiation from the model results shows the potential for restoration in some areas of the catchment. Other components of the atmospheric heat budget depend on climate conditions, which are assumed to be spatially uniform for this model. Climate change scenarios could be performed using this model to see how other atmospheric components could impact stream temperature under different climatic conditions.

Acknowledgements

This research was financed by the Danish Research Counsel as part of the RISKPOINT project and by the Danish Hydraulic Institute. We would like to thank Dayna Gross and Robert Unnasch of The Nature Conservancy in the Silver Creek Preserve and Boise, Idaho, Kevin Lakey of Water Master District 37 in Shoshone, Idaho, Lin Campbell of the Idaho Department of Water Resources, David Tuthill and Lee Brown of Idaho Water Engineering, and the Wood River Valley property owners for their help in our field data collection efforts and kind support. The support of Professor Peter Goodwin, Director of the Center for Ecohydraulics Research, University of Idaho is also gratefully acknowledged.

Supplementary material

Supplementary data (Appendix A, B and C) associated with this article can be found, in the online version, at http://dx.doi.org/10.1016/j.jhydrol.2013.04.039.

References

Allan, J.D., Castillo, M.M., 2007. Stream Ecology: Structure and Function of Running Waters, second ed. Springer, Dordrecht, The Netherlands.

Allen, G.R., Pereira, L.S., Raes, D., Martin, S., 1998. Crop Evapotranspiration – Guidelines for Computing Crop Water Requirements. FAO Irrigation and Drainage Paper 56, p. 300.

Arya, S.P., 2001. Introduction to Micrometeorology, second ed. Academic Press, San Diego.

Bartolino, J.R., 2009. Ground-water Budgets for the Wood River Valley Aquifer System, South-Central Idaho, 1995–2004. U.S. Geological Survey Scientific Investigations Report 2007-5258, 36p.

Beschta, R.L., 1997. Riparian shade and stream temperature: an alternative perspective. Rangelands 19 (2), 25–28.

Bogan, T., Mohseni, O., Stefan, H.G., 2003. Stream temperature–equilibrium temperature relationship. Water Resour. Res. 39 (9), 1245–1257.

Boyd, M., Kasper, B., 2003. Analytical Methods for Dynamic Open Channel Heat and Mass Transfer: Methodology for Heat Source Model Version 7.0. <http://www.deq.state.or.us/wq/tmdls/docs/tools/heatsourcemanual.pdf>.

Bredehoeft, J.D., Papadopulos, I.S., 1965. Rates of vertical groundwater movement estimated form the earth's thermal profile. Water Resour. Res. 1 (2), 325–328.

Brockway, C.E., Grover, K.P., 1978. Evaluation of Urbanization and Changes in Land Use on the Water Resources of Mountain Valleys: Moscow, University of Idaho Water Resources Research Institute, Research Technical Completion Report, Project B-038-IDA, 104p.

Brockway, C.E., Kahlown, M.A., 1994. Hydrologic Evaluation of the Big Wood River and Silver Creek Watersheds Phase I: Kimberly. University of Idaho Water Resources Research Institute, Kimberly Research Center, 53p.

Butts, M.B., Kristensen, M., Payne, J.T., Madsen, H., 2004. An evaluation of the impact of model structure on hydrological modelling uncertainty for streamflow prediction. J. Hydrol. 298 (1–4), 242–266, 1 October 2004.

Butz, B.P., Schregardus, D.R., Lewis, B., Policastro, A.J., Reisa, J.J., 1974. Ohio River Cooling Water Study. Argonne National Laboratory, Environmental Protection Agency, EPA-905/9-74-004.

Cassie, D., 2006. The thermal regime of rivers: a review. Freshw. Biol. 51, 1389–1406.

Chapra, S.C., 1997. Surface Water-Quality Modeling. McGraw-Hill, New York.

Chapra, S.C., Canale, R.P., 1998. Numerical Methods for Engineers: With Programming And Software Applications, third ed. McGraw-Hill, Boston.

Chen, Y.D., Carsel, R.F., McCutcheon, S.C., Nutter, W.L., 1998. Stream temperature simulation of forested riparian areas: I. Watershed scale model development. J. Environ. Eng. 124 (4), 304–315.

Constantz, J., 2008. Heat as a tracer to determine streambed water exchanges. Water Resour. Res. 44, W00D10. http://dx.doi.org/10.1029/2008WR006996.

DHI, 2009a. MIKE SHE User Manual, vol. 2. Reference Guide. MIKE by DHI 2009.

DHI, 2009b. MIKE11 – A Modelling System for Rivers and Channels, Reference Manual. MIKE by DHI 2009.

DHI, 2009c. ECO LAB: Short Scientific Description. MIKE by DHI 2009.

Domenico, P.A., Schwartz, F.W., 1998. Physical and Chemical Hydrogeology, second ed. John Wiley and Sons Inc., New York.

Ecosystem Sciences Foundation, 2011. Silver Creek Watershed: An Ecological Enhancement Strategy for Silver Creek, Idaho. Prepared for: The Nature Conservancy.

ET Idaho, 2010. Evapotranspiration and Consumptive Irrigation Water Requirements for Idaho. University of Idaho Research and Extension Center at Kimberly, Idaho. <http://www.kimberly.uidaho.edu/ETIdaho/>.

Fujimoto, Y., Ouchi, Y., Hakuba, T., Chiba, H., Iwata, M., 2008. Influence of modern irrigation, drainage system and water management on spawning migration of mud loach, *Misgurnus anguillicaudatus* C. Environ. Biol. Fishes (81), 185–194.

Gillilan Associates, Inc., 2007. Kilpatrick Pond and Dam Restoration Feasibility Study – Final Report. Prepared for: The Nature Conservancy.

Graham, D.N., Butts, M.B., 2006. Flexible, integrated watershed modelling with MIKE SHE. In: Singh, V.P., Frevert, D.K. (Eds.), Watershed Models. CRC Press, pp. 245–272, ISBN: 084933609.

Gu, R., Montgomery, S., Austin, T.A., 1998. Quantifying the effects of stream discharge on summer river temperature. Hydrol. Sci. J. 43 (6), 885–904.

Haper, D., Pacini, N., Zalewski, M., 2008. Ecohydrology: Processes, Models and Case Studies. CAB International, Wallinford, UK, 391 pp.

Hill, M.C., 1998. Methods and Guidelines for Effective Model Calibration. US Geological Survey Water Resources Investigations Report 98-4005.

Hock, R., 2003. Temperature index melt modelling in mountain areas. J. Hydrol. 282 (1–4), 104–115.

Idaho Department of Water Resources, 2010. Well Drillers Reports. <http://www.idwr.idaho.gov/WaterManagement/WellInformation/DrillerReports/dr_default.htm.>

Jackman, A.P., Yotsukura, N., 1977. Thermal Loading of Natural Streams. US Geological Survey Professional Paper 991.

Kennedy, E.J., 1984. Discharge Ratings at Gaging Stations. U.S. Geological Survey Techniques of Water-Resources Investigations, 59p, book 3 (Chapter A10).

Kim, K.S., Chapra, S.C., 1997. Temperature model for highly transient shallow streams. J. Hydraul. Eng. 123 (1), 30–40.

Kinzelbach, W.K., 1981. Managing the cooling capacity of the upper rhine. Environ. Manage. 5 (1), 69–77.

Klein, L.R., Clayton, S.R., Alldredge, J.R., Goodwin, P., 2007. Long-term monitoring and evaluation of the lower red river meadow restoration project, Idaho, U.S.A. Restor. Ecol. 15 (2), 223–239.

Larson, L.L., Larson, S.L., 1996. Riparian shade and stream temperature: a perspective. Rangelands 18 (4), 149–152.

Lowney, C.L., 2000. Stream temperature variation in regulated rivers: evidence for a spatial pattern in daily minimum and maximum magnitudes. Water Resour. Res. 36 (10), 2947–2955.

Moreland, J.A., 1977. Ground water–surface water relations in the Silver Creek area, Blaine county, Idaho: Boise, Idaho Department of Water Resources. Water Inform. Bull. 44, 42p.

Nielsen, S.A., Hansen, E., 1973. Numerical simulation of the rainfall runoff process on a daily basis. Nord. Hydrol. 4, 171–190.

Penman, H.L., 1948. Natural evaporation from open water, bare soil, and grass. Roy. Soc. Lond. Proc. Ser. A Math. Phys. Sci. 193 (1032), 120–145.

Poulin, M., Hubert, P., 1982. Une Méthode de Calcul de l'Echauffement des Rivières – Application à la Gestion des Rejets Thermiques au Rhin. J. Hydrol. 55, 195–211.

Refsgaard, J.C., Storm, B., 1995. MIKE SHE. In: Singh, V.P. (Ed.), Computer Models of Watershed Hydrology. Water Resources Publications, pp. 809–846.

Refsgaard, J.C., Støm, B., Clausen, T., 2010. Système Hydrologique Europeen (SHE): review and perspectives after 30 years development in distributed physically-based hydrological modelling. Hydrol. Res. 41 (5), 355–377.

Roth, T.R., Westhoff, M.C., Huwald, H., Huff, J.A., Rubin, J.F., Barrenetxea, G., Vetterli, M., Parriaux, A., Selker, J.S., Parlange, M.B., 2010. Stream temperature response to three riparian vegetation scenarios by use of a distributed temperature validated model. Environ. Sci. Technol. 44 (6), 2072–2078.

Runkel, R.L., 1996. Solution of the advection–dispersion equation: continuous load of finite duration. J. Environ. Eng. 122 (9), 830–832.

Saucer, V.B., Meyer, R.W., 1992. Determination of error in individual discharge measurements. US Geological Survey Open-File Report 92-144, 21p.

Sellers, W.D., 1965. Physical Climatology. University of Chicago Press, Chicago, IL, 272pp.

Shanley, J.B., Peters, N.E., 1988. Preliminary observations of streamflow generation during storms in a forested piedmont watershed using temperature as a tracer. J. Contam. Hydrol. 3, 349–365.

Sinokrot, B.A., Stephan, H.G., 1993. Stream temperature dynamics: measurements and modeling. Water Resour. Res. 29 (7), 2299–2312.

Sinokrot, B.A., Gulliver, J.S., 2000. In-stream flow impact on river water temperatures. J. Hydraul. Res. 38 (5), 339–349.

Skinner, K.D., Bartolino, J.R., Tranmer, A.W., 2007. Water-resource Trends and Comparisons between Partial Development and October 2006 Hydrologic

Conditions. Wood River Valley, South-central Idaho: U.S. Geological Survey Scientific Investigations Report 2007-5258, 30p.
Thomann, R.V., Mueller, J.A., 1987. Principles of Surface Water Quality Modeling and Control. Harper & Row Publishers, Inc., New York.
Thompson, J.R., Sørenson, H.R., Gavin, H., Refsgaard, A., 2004. Application of the coupled MIKE SHE/MIKE 11 modelling system to a lowland wet grassland in southeast England. J. Hydrol. 293, 151–179.
TNC, 2011. Personal Communication with the Nature Conservancy Field Staff.
US Bureau of Reclamation, 2010. The Pacific Northwest Cooperative Agricultural Weather Network – AgriMet Weather Data. <http://www.usbr.gov/pn/agrimet/wxdata.html>.
US Department of Agriculture, 2010. Natural Resource Conservation Service. <http://www.nrcs.usda.gov/wps/portal/nrcs/main/national/soils>.
US Geological Survey, 2010a. National Water Information System: Web Interface. <http://waterdata.usgs.gov/nwis>.
US Geological Survey, 2010b. National Land Cover Dataset. <http://www.mrlc.gov/index.asp>.
US Geological Survey, 2010c. National Hydrography Dataset. <http://nhd.usgs.gov/>.
US Geological Survey, 2010d. StreamStats. <http://water.usgs.gov/osw/streamstats/>.
Viswanadham, Y., Ramanadham, R., 1970. Estimation of long wave radiation by an empirical method. Pure Appl. Geophys. 81, 272–278.
Water District 37 and 37-M, 1999. Annual Report 1999 Water Distribution and Hydrometric Works in Water District 37 Big Wood River and Water District 37-M Little Wood River-Silver Creek: Shoshone, Idaho, Water District 37 and 37-M.
Webb, B.W., Clack, P.D., Walling, D.E., 2003. Water–air temperature relationships in a Devon river system and the role of flow. Hydrol. Process. 17, 3069–3084.
Westhoff, M.C., Savenije, H.H.G., Luxemburg, W.M.J., Stelling, G.S., van de Giesen, N.C., Selker, J.S., Pfister, L., Uhlenbrook, S., 2007. A distributed stream temperature model using high resolution temperature observations. Hydrol. Earth Syst. Sci. 11, 1469–1480.
Wetzstein, A.B., Robinson, C.W., Brockway, C.E., 2000. Hydrologic Evaluation of the Big Wood River and Silver Creek Watersheds, Phase II: Kimberly. University of Idaho Water Resources Research Institute, Kimberly Research Center, Idaho, 136p.
Wissmar, R.C., Beschta, R.L., 1998. Restoration and management of riparian ecosystems: a catchment perspective. Freshw. Biol. 40, 151–179.
Yan, J., Smith, K.R., 1994. Simulation of integrated surface water and ground water systems – model formulation. Water Resour. Bull. 30 (5), 879–890.
Younus, M., Hondzo, M., Engel, B.A., 2000. Stream temperature dynamics in upland agricultural watersheds. J. Environ. Eng. 126 (6), 518–526.
Zalewski, M., 2000. Ecohydrology – the scientific background to use ecosystem properties as management tools toward sustainability of water resources. Ecol. Eng. 16, 1–8.